

A. Boumassata, D. Kerdoun, O. Oualah

Maximum power control of a wind generator with an energy storage system to fix the delivered power

Introduction. The power extracted from the wind turbine and delivered to the electrical network must be maximum and constant and the whole system should have a good compromise between efficiency and cost. In order to attenuate this objective, a doubly fed induction machine, a cycloconverter, a maximum power point tracking algorithm and a flywheel energy storage system constitute a very interesting solution among many others that have been proposed. **Novelty.** The novelty of the proposed work is to use a doubly fed induction machine and a three pulses cycloconverter to reduce the cost and to integrate a flywheel energy storage system between the wind generator and the electrical network to maintain the constancy of the power sent to the network, following the instability of the wind. The proposed work uses a maximum power point tracking algorithm to capture the optimal power available in the wind in order to increase the efficiency of the system. **Results.** A detailed study of the proposed system is presented with the detailed dynamic modeling equations and simulation results are conducted to show the performance and the efficiency of the suggested work. References 21, figures 15.

Key words: maximum power point tracking, flywheel energy storage system, doubly fed induction machine, cycloconverter.

Вступ. Потужність, що видобувається з вітряної турбіни і подається в електричну мережу, має бути максимальною і постійною, а вся система повинна мати хороший компроміс між ефективністю та вартістю. Щоб пом'якшити це завдання, асинхронна машина з подвійним живленням, дуже цікавим рішенням серед багатьох інших, які були запропоновані, є циклоконвертер, алгоритм відстеження точки максимальної потужності та система накопичення енергії маховика. **Новизна.** Новизна запропонованої роботи полягає у використанні асинхронної машини з подвійним живленням та трімппульсного циклоконвертера для зниження вартості та інтеграції маховикової системи накопичення енергії між вітрогенератором та електричною мережею для підтримки сталості потужності, що відправляється в мережу, враховуючи нестабільність вітру. Запропонована робота використовує алгоритм відстеження точки максимальної потужності для захоплення оптимальної потужності, доступної на вітру, щоб підвищити ефективність системи. **Результати.** Детальне дослідження запропонованої системи представлено з докладними рівняннями динамічного моделювання, а результати проведеного моделювання показують продуктивність та ефективність запропонованої роботи. Бібл. 21, рис. 15.

Ключові слова: відстеження точки максимальної потужності, система накопичення енергії маховика, асинхронна машина з подвійним живленням, циклоконвертер.

Introduction. Wind energy is the fastest growing energy among the new power generation sources in the world [1]. The most important machine used in wind turbine generators for wind energy conversion system is the doubly fed induction machine (DFIM).

The DFIM is an induction machine with wound rotor. It can function like motor or generator. The principal advantage of this machine is that the converter on the rotor side uses 20-30 % of the rated power [2].

Among the converters which make directly the conversion of power without any intermediary of a continuous bus, is the cycloconverter. This converter contains thyristors which make the system less expensive. Cycloconverter is habitually used in large power applications like rolling mills [3, 4], electric traction [5], static Scherbius drives [6] and more. The three pulses cycloconverter is our choice to control the DFIM in both systems (wind generator and flywheel energy storage system (FESS)).

The **purpose** of this work is to extract the maximum power available in the wind and to provide it to the electrical network as a constant as possible with good compromise between cost and efficiency.

In works [7, 8] a flywheel with an asynchronous machine have been integrated between the wind generator and the grid and controlled via an AC-DC-AC converter. In article [9] the author used a flywheel and a synchronous machine as a storage system and controlled by an AC-DC-AC converter. So, in order to achieve this purpose we used, a DFIM and a three pulses

cycloconverter to reduce the cost and to support more current, a FESS between the wind generator and the network to maintain the constancy and to prove the quality of the power sent to the network following the instability of the wind, and a maximum power point tracking algorithm to capture the optimal power available in the wind to increase the efficiency of the whole system.

Figure 1 shows the configuration of the proposed and studied system.

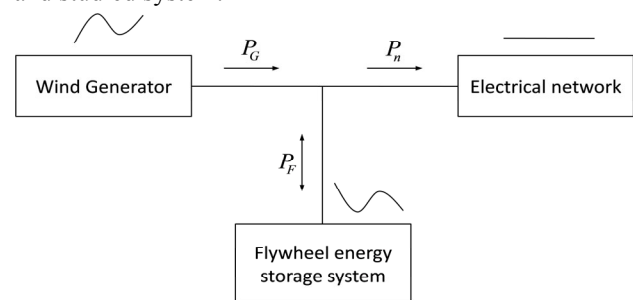


Fig. 1. Studied model

Modeling of the turbine. The mechanical power of the wind turbine P_t is written as [10-12]:

$$P_t = \frac{1}{2} \cdot \rho \cdot R \cdot C_p(\lambda, \beta) \cdot V^3, \quad (1)$$

where ρ , R , C_p , λ , β and V are respectively the air density, turbine radius, power coefficient, tip speed ratio, pitch angle and the speed of the wind.

C_p is the wind turbine aerodynamic efficiency. It depends on λ and β , where λ is written as:

$$\lambda = \frac{\Omega_t \cdot R}{V}, \quad (2)$$

where Ω_t is the speed of the turbine.

The power coefficient is defined as [13]:

$$C_p(\lambda, \beta) = (0.35 - 0.00167(\beta - 2)) \cdot \sin\left(\frac{\pi \cdot (\lambda + 0.1)}{14.34 - 0.3(\beta - 2)}\right) - 0.00184(\lambda - 3) \cdot (\beta - 2). \quad (3)$$

Figure 2 shows the curve of C_p obtained via (3). The optimal value of C_p ($C_{pmax} = 0.35$) is for $\lambda = 7.1$ and $\beta = 2^\circ$.

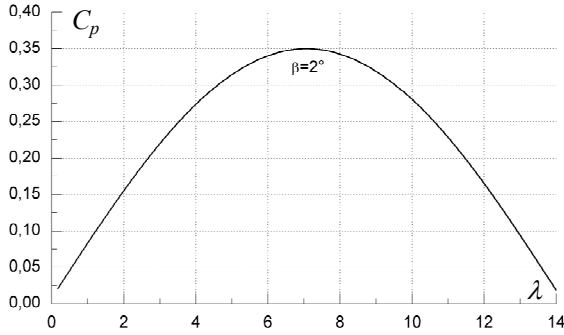


Fig. 2. C_p of the wind turbine

The expression of the mechanical equation is described as follows:

$$J \frac{d\Omega_{mec}}{dt} = T_m - T_{em} - f \cdot \Omega_{mec}, \quad (4)$$

where J , f are the equivalent inertia and friction coefficient, respectively; Ω_{mec} is the generator's mechanical speed; T_{em} and T_m are the electromagnetic torque and the torque of the turbine referred to the generator, respectively.

Optimal power control. The optimal power characteristics of the wind turbine are strongly nonlinear. For each wind speed (Fig. 3), the system must find the maximum power of what is equivalent to search for the optimal rotor speed (mechanical speed).

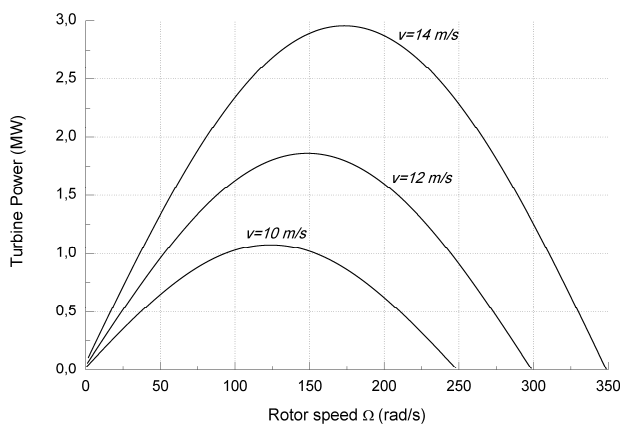


Fig. 3. Power-speed characteristics for different wind speeds

If the rotor speed does not reach its optimal value, the power of the turbine will not be able to reach the optimal power any more. It is possible to regulate the torque of the generator (electromagnetic torque) so as to control the rotor speed so that this one varies with the change of the wind speed (Fig. 4).

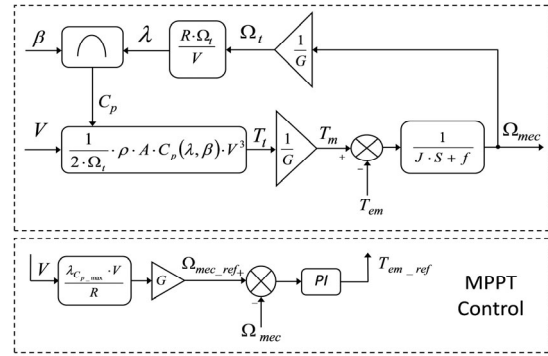


Fig. 4. Optimal power control

From Fig. 4 we can write the reference power as follows:

$$P_{ref} = T_{em_ref} \cdot \Omega_{mec}. \quad (5)$$

According to the maximum power point tracking (MPPT) control strategy, the reference power has been generated and delivered to the generator control system, which compares the reference power with the measured output power from the generator to produce the control signals for the power converter. Through the control of the converter, the electrical power of the generator will be equal to its reference, at which the maximum power operation will be achieved.

Modeling of the cycloconverter. The three phase cycloconverter is constituted of 18 thyristors. Each phase is constituted of two converters. The delay angles of those converters are modulated so as to supply an AC output voltage at the required magnitude and frequency.

Figure 5 illustrates the model of three phase-three phase cycloconverter. The function of the switches (Fig. 5) is described as:

$$S_{K_{ij}} = \begin{cases} 1 & S_{K_{ij}} \text{ is closed;} \\ 0 & S_{K_{ij}} \text{ is open,} \end{cases} \quad (6)$$

where $K \in \{P, N\}$, $i \in \{a, b, c\}$, and $j \in \{A, B, C\}$.

The voltages equation at the output of the three phase cycloconverter can be written in function of $[T]$ as follows [14]:

$$\begin{bmatrix} v_A \\ v_B \\ v_C \end{bmatrix} = [T] \cdot \begin{bmatrix} v_a \\ v_b \\ v_c \end{bmatrix}; \quad (7)$$

Fig. 5. Three-phase cycloconverter

$$[T] = \begin{bmatrix} (S_{P_{aA}} + S_{N_{aA}}) & (S_{P_{bA}} + S_{N_{bA}}) & (S_{P_{cA}} + S_{N_{cA}}) \\ (S_{P_{aB}} + S_{N_{aB}}) & (S_{P_{bB}} + S_{N_{bB}}) & (S_{P_{cB}} + S_{N_{cB}}) \\ (S_{P_{aC}} + S_{N_{aC}}) & (S_{P_{bC}} + S_{N_{bC}}) & (S_{P_{cC}} + S_{N_{cC}}) \end{bmatrix} \quad (8)$$

where v_a , v_b and v_c are the input voltages; v_A , v_B and v_C are the output voltages.

The voltages at the output of the cycloconverter are commanded using cosine-wave crossing control to produce the firing pulses of the switches. So we will have

three reference waves and three timing waves and a lot of intersection points. We will have 18 control circuits for this cycloconverter one for each switch [14].

Modeling of the DFIM. The electrical expressions of the DFIM are written as [15, 16]:

$$\begin{cases} V_{sdq} = R_s \cdot I_{sdq} + \frac{d\phi_{sdq}}{dt} \mp \dot{\theta}_s \cdot \phi_{sqd}; \\ V_{rdq} = R_r \cdot I_{rdq} + \frac{d\phi_{rdq}}{dt} \mp \dot{\theta}_r \cdot \phi_{rqd}; \end{cases} \quad (9)$$

$$\begin{cases} \phi_{sdq} = L_s \cdot I_{sdq} + M \cdot I_{rqd}; \\ \phi_{rdq} = L_r \cdot I_{rdq} + M \cdot I_{sqd}, \end{cases} \quad (10)$$

where R_s and R_r are the stator and rotor phase resistances; θ_s and θ_r are the stator and rotor field angles; L_s , L_r and M are the cyclic stator, rotor and mutual inductances, respectively.

The expressions of the active and reactive powers at the output of the DFIM are given as:

$$\begin{cases} P = P_s + P_r; \\ Q = Q_s + Q_r, \end{cases} \quad (11)$$

where P_s , Q_s , P_r and Q_r are the stator (rotor) active and reactive powers, respectively.

The equation of the electromagnetic torque is:

$$T_{em} = p \cdot (\phi_{sd} \cdot I_{sq} - \phi_{sq} \cdot I_{sd}), \quad (12)$$

where p is the pole pairs number.

Control of the DFIM. For controlling independently the active and reactive powers of the DFIM, the stator flux vector will be aligned with d-axis ϕ_{sd} ($\phi_{sd} = \phi_s$ and $\phi_{sq} = 0$) [17-19] and the expressions of the stator voltages are given by:

$$\begin{cases} V_{sd} = 0; \\ V_{sq} = V_s. \end{cases} \quad (13)$$

The rotor flux equations can be written as:

$$\begin{cases} \phi_{rd} = \sigma \cdot L_r \cdot I_{rd} + \frac{M}{L_s} \cdot \phi_{sd}; \\ \phi_{rq} = \sigma \cdot L_r \cdot I_{rq}, \end{cases} \quad (14)$$

with

$$\sigma = 1 - \frac{M^2}{L_s \cdot L_r}, \quad (15)$$

where σ is the leakage coefficient.

We can write the voltages at the rotor according to the rotor currents as follows:

$$\begin{cases} V_{rd} = R_r \cdot I_{rd} + \sigma \cdot L_r \cdot \frac{dI_{rd}}{dt} - s \cdot \omega_s \cdot \sigma \cdot L_r \cdot I_{rq}; \\ V_{rq} = R_r \cdot I_{rq} + \sigma \cdot L_r \cdot \frac{dI_{rq}}{dt} + s \cdot \omega_s \cdot \sigma \cdot L_r \cdot I_{rd} + s \cdot \frac{M \cdot V_s}{L_s}, \end{cases} \quad (16)$$

where s is the machine slip.

The simplified formula of the electromagnetic torque is given as follows:

$$T_{em} = -p \cdot \frac{M}{L_s} \cdot \phi_{sd} \cdot I_{rq}. \quad (17)$$

The expressions of the DFIM powers at the stator are written as follows:

$$\begin{cases} P_s = -V_s \cdot \frac{M}{L_s} \cdot I_{rq}; \\ Q_s = \frac{V_s^2}{\omega_s \cdot L_s} - V_s \cdot \frac{M}{L_s} \cdot I_{rd}, \end{cases} \quad (18)$$

We can simplify the expressions of the output powers of the DFIM as follows:

$$\begin{cases} P = (s-1) \cdot V_s \cdot \frac{M}{L_s} \cdot I_{rq}; \\ Q = \frac{V_s^2}{\omega_s \cdot L_s} + (s-1) \cdot V_s \cdot \frac{M}{L_s} \cdot I_{rd}. \end{cases} \quad (19)$$

The DFIM and the flywheel are the main parts of the flywheel energy storage system. This system stores energy in kinetic form and provides it in electrical form; in other words, the FESS stores energy in kinetic form in the flywheel during motor mode and it provides energy in electrical form during generator mode.

The kinetic energy stocked in the flywheel is defined as follows [9]:

$$E = \frac{1}{2} \cdot J_F \cdot \Omega_F^2 \quad (20)$$

or

$$E = \int P_M \cdot dt, \quad (21)$$

where J_F is the flywheel inertia; Ω_F is flywheel mechanical speed; P_M is the electrical power.

The reference active power provided to the network/FESS from the wind generator is determined by (5) (Fig. 4), and it's written as follows:

$$P_{G_ref} = T_{em_ref} \cdot \Omega_{mec}. \quad (22)$$

The expression of the reference active power (electrical power of the FESS) is determined from the difference between the desired power provided to the network and the power generated through the wind generator:

$$P_{M_ref} = P_{n_ref} - P_{G_ref}. \quad (23)$$

The suggested system contains two control blocks: wind generator control block (Fig. 6) and FESS control block (Fig. 7). The first block is devoted to controlling the power provided from the wind generator to the network/FESS; when the power provided to the network from the wind generator is more than the required power at the network, the rest of this power is transferred to the FESS and stocked in the flywheel. The second block is devoted to controlling the power exchanged between the FESS and the network; the FESS stores the power from the wind generator and provides it to the network if the required power of the network is not enough.

The powers' expressions delivered to the network are written as:

$$\begin{cases} P_n = P_G + P_M; \\ Q_n = Q_G + Q_M. \end{cases} \quad (24)$$

The detailed control schemes of the DFIM in both wind generator and FESS are illustrated respectively in Fig. 6, 7.

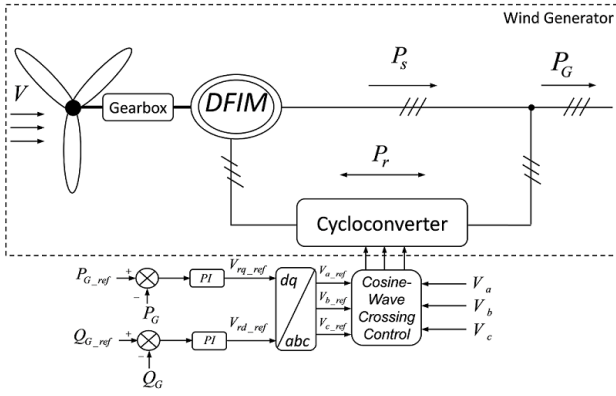


Fig. 6. Wind generator control block

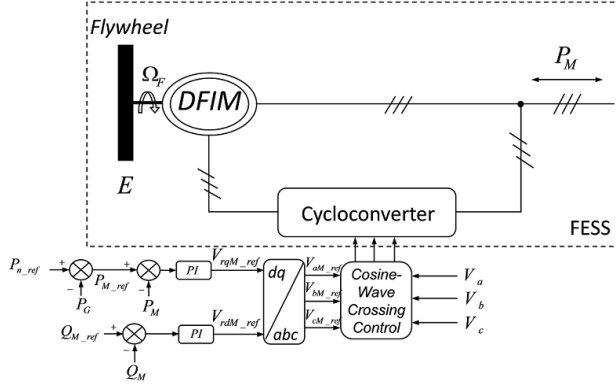


Fig. 7. Wind FESS control block

Simulation results. The model introduced in Fig. 1 was simulated under MATLAB/Simulink and its parameters are given as follows:

- wind generator [20]: number of blades = 3; gear box $G = 70$; blade radius $R = 40$ m; $S_n = 3$ MVA; $U_s = U_r = 690$ V; $f = 50$ Hz; $R_s = 2.97$ m Ω ; $R_r = 3.82$ m Ω ; $L_s = 12.241$ mH; $L_r = 12.177$ mH; $M = 12.12$ mH; $J = 116$ kg m 2 ; $p = 2$.

- DFIM (used in the FESS) [21]: $S_n = 1.5$ MVA; $R_s = 0,012$ Ω ; $R_r = 0,021$ Ω ; $L_s = 13,7037$ mH; $L_r = 13,6751$ mH; $M = 13,5$ mH; $f = 0,0024$; $p = 2$; $J_F \approx 351.5$ kg m 2 .

The network requires a constant power of -1.5 MW (the negative value indicates that the network receive power).

The flywheel inertia value was calculated for a speed range between 120 rad/s and 200 rad/s during 3 s and the rated power is 1.5 MW.

Figures 8,*a,b* demonstrate the operation of the energy storage system.

The initial value of the rotor speed must be corresponding to the initial value of the wind speed.

The generator speed (Fig. 10) follows its reference and varies according to the wind speed variations (Fig. 9). This figure checks the MPPT control.

The active powers of the wind generator and the FESS (Fig. 11,*a,b*) follow their references correctly. The active power provided to the network given in Fig. 12,*a* is constant at -1.5 MW and the reactive power (Fig. 12,*b*) is zero for ensuring unity power factor.

Figure 13 shows the zoom of the voltage and current in the rotor side (FESS) and confirms the control of the cycloconverter.

The speed of the flywheel (Fig. 14) increases when the energy is stored and decreases when the energy is provided (Fig. 15).

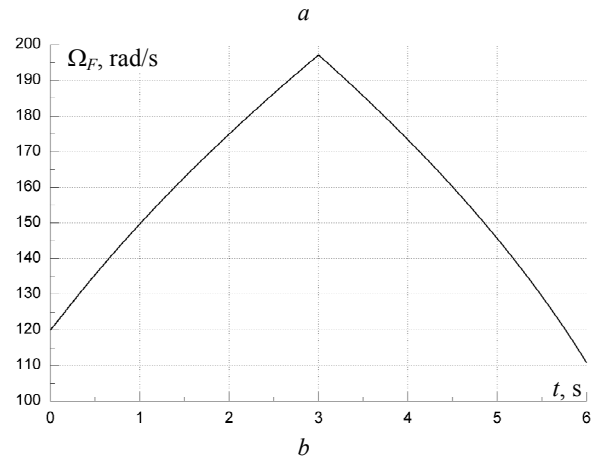
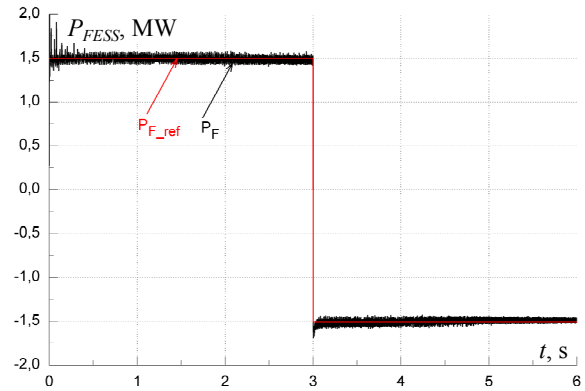


Fig. 8. Active power (*a*) and mechanical speed (*b*) of the FESS

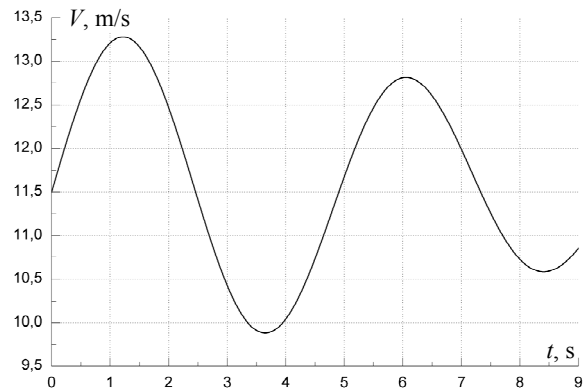


Fig. 9. Wind speed

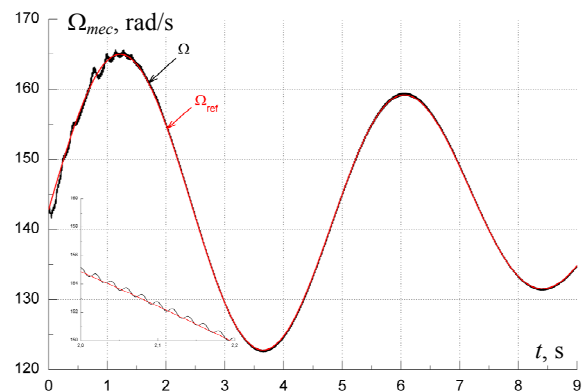


Fig. 10. Generator speed (wind generator)

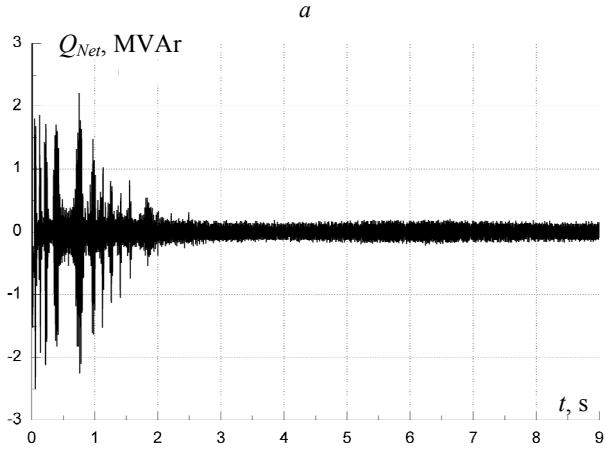
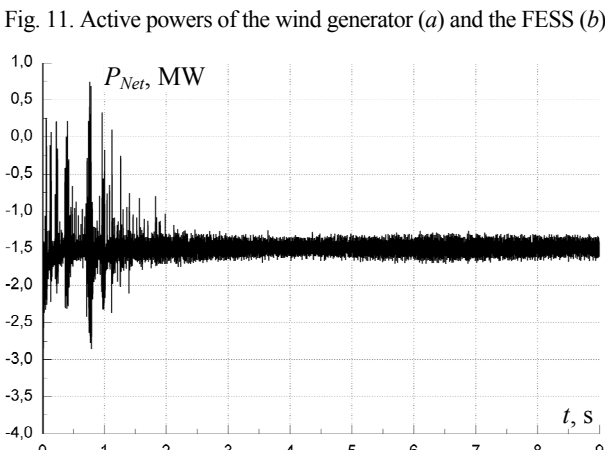
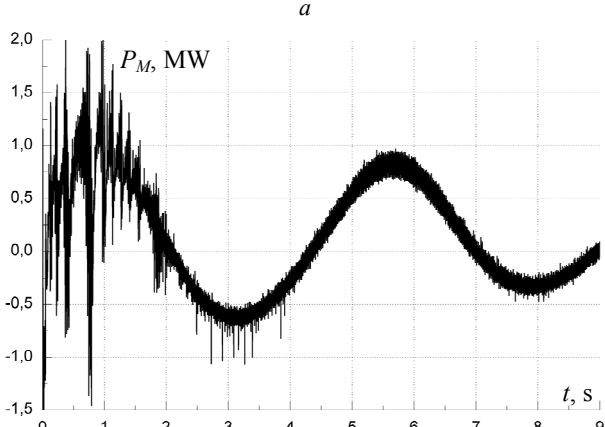
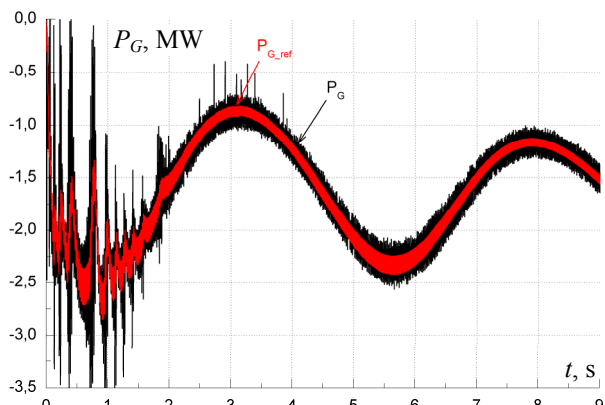


Fig. 12. Network powers

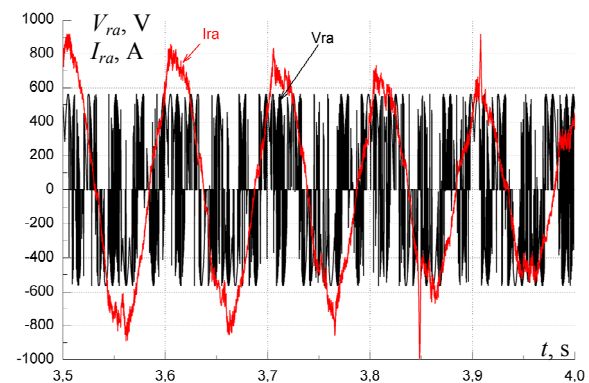


Fig. 13. Rotor phase voltage and current of the DFIM (FESS)

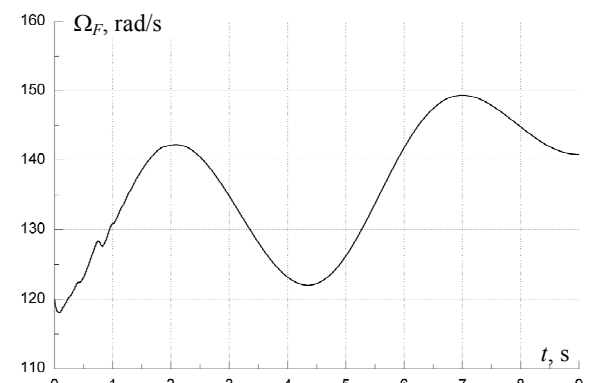


Fig. 14. Speed of the flywheel

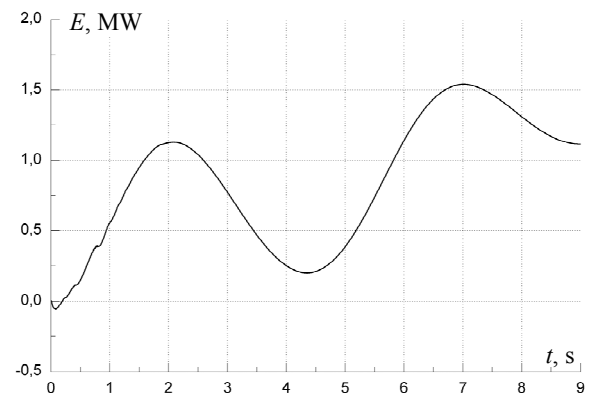


Fig. 15. Energy stocked in the flywheel

Conclusion.

In this article, the wind generator attached with a flywheel energy storage system was studied for different wind speed. The storage system based on doubly fed induction machine and three pulses cycloconverter has been controlled through a reference power as a function of a power generator and a desired network power. Simulation results show, firstly, that the extraction of the maximum power using maximum power point tracking control algorithm was well done. Secondly, they show that the flywheel energy storage system has been capable to store and provide energy, to ensure that the power sent to the electrical network remains constant. Finally, they demonstrate that the wind power fluctuations can be mostly compensated via the storage system. So, the performance and the efficiency of the suggested work have been verified.

Conflict of interest. The authors declare that they have no conflicts of interest.

REFERENCES

1. Beltran B., Ahmed-Ali T., Benbouzid M. High-Order Sliding-Mode Control of Variable-Speed Wind Turbines. *IEEE Transactions on Industrial Electronics*, 2009, vol. 56, no. 9, pp. 3314-3321. doi: <https://doi.org/10.1109/TIE.2008.2006949>.
2. Longya Xu, Wei Cheng. Torque and reactive power control of a doubly fed induction machine by position sensorless scheme. *IEEE Transactions on Industry Applications*, 1995, vol. 31, no. 3, pp. 636-642. doi: <https://doi.org/10.1109/28.382126>.
3. Timpe W. Cycloconverter Drives for Rolling Mills. *IEEE Transactions on Industry Applications*, 1982, vol. IA-18, no. 4, pp. 400-404. doi: <https://doi.org/10.1109/TIA.1982.4504099>.
4. Hagmann R. AC-cycloconverter drives for cold and hot rolling mill applications. *Conference Record of the 1991 IEEE Industry Applications Society Annual Meeting*, 1991, pp. 1134-1140. doi: <https://doi.org/10.1109/IAS.1991.178005>.
5. Jacovides L.J., Matouka M.F., Shimer D.W. A Cycloconverter - Synchronous Motor Drive for Traction Applications. *IEEE Transactions on Industry Applications*, 1981, vol. IA-17, no. 4, pp. 407-418. doi: <https://doi.org/10.1109/TIA.1981.4503968>.
6. Smith G.A. Static Scherbius system of induction-motor speed control. *Proceedings of the Institution of Electrical Engineers*, 1977, vol. 124, no. 6, p. 557. doi: <https://doi.org/10.1049/ptee.1977.0114>.
7. Davigny A. *Participation aux services système de fermes d'éoliennes à vitesse variable intégrant du stockage inertiel d'énergie*. Thèse de doctorat, Hautes Études d'Ingénieur, 2007. (Fra).
8. Cimuca G.O. *Système inertiel de stockage d'énergie associé à des générateurs éoliens*. PhD Dissertation, Lille, ENSAM, 2005. (Fra).
9. Leclercq L. *Apport du stockage inertiel associé à des éoliennes dans un réseau électrique en vue d'assurer des services systèmes*. University of Lille in France, 2004. (Fra).
10. Boutoubat M., Mokrani L., Machmoum M. Control of a wind energy conversion system equipped by a DFIG for active power generation and power quality improvement. *Renewable Energy*, 2013, vol. 50, pp. 378-386. doi: <https://doi.org/10.1016/j.renene.2012.06.058>.
11. Tang C.Y., Guo Y., Jiang J.N. Nonlinear Dual-Mode Control of Variable-Speed Wind Turbines With Doubly Fed Induction Generators. *IEEE Transactions on Control Systems Technology*, 2011, vol. 19, no. 4, pp. 744-756. doi: <https://doi.org/10.1109/TCST.2010.2053931>.
12. El-Sattar A.A., Saad N.H., El-Dein M.Z.S. Dynamic response of doubly fed induction generator variable speed wind turbine under fault. *Electric Power Systems Research*, 2008, vol. 78, no. 7, pp. 1240-1246. doi: <https://doi.org/10.1016/j.eprsr.2007.10.005>.
13. Gaillard A. *Système éolien basée sur une mada: contibution à l'étude de la qualité de l'énergie électrique et de la continuité de service*. PhD Dissertation, Nancy, 2010. (Fra).
14. Boumassata A., Kerdoun D. Modeling, Simulation and Control of Wind Energy Conversion System based on Doubly Fed Induction Generator and Cycloconverter. *Advances in Electrical and Computer Engineering*, 2014, vol. 14, no. 2, pp. 43-48. doi: <https://doi.org/10.4316/AECE.2014.02007>.
15. Kairous D., Wamkeue R. DFIG-based fuzzy sliding-mode control of WECS with a flywheel energy storage. *Electric Power Systems Research*, 2012, vol. 93, pp. 16-23. doi: <https://doi.org/10.1016/j.eprsr.2012.07.002>.
16. Kassem A.M., Hasaneen K.M., Yousef A.M. Dynamic modeling and robust power control of DFIG driven by wind turbine at infinite grid. *International Journal of Electrical Power & Energy Systems*, 2013, vol. 44, no. 1, pp. 375-382. doi: <https://doi.org/10.1016/j.ijepes.2011.06.038>.
17. Poitiers F. *Etude et commande de génératrices asynchrones pour l'utilisation de l'énergie éolienne-machine asynchrone à cage autonome-machine asynchrone à double alimentation reliée au réseau*. PhD Dissertation, Université de Nantes, 2003. (Fra).
18. Bekakra Y., Ben Attous D. Sliding mode controls of active and reactive power of a DFIG with MPPT for variable speed wind energy conversion. *Australian Journal of Basic and Applied Sciences*, 2011, vol. 5, no. 12, pp. 2274-2286. Available at: <http://www.ajbasweb.com/old/ajbas/2011/December-2011/2274-2286.pdf> (Accessed 11 May 2021).
19. Jerbi L., Krichen L., Ouali A. A fuzzy logic supervisor for active and reactive power control of a variable speed wind energy conversion system associated to a flywheel storage system. *Electric Power Systems Research*, 2009, vol. 79, no. 6, pp. 919-925. doi: <https://doi.org/10.1016/j.eprsr.2008.12.006>.
20. Gaillard A., Poure P., Saadate S., Machmoum M. Variable speed DFIG wind energy system for power generation and harmonic current mitigation. *Renewable Energy*, 2009, vol. 34, no. 6, pp. 1545-1553. doi: <https://doi.org/10.1016/j.renene.2008.11.002>.
21. El Aïmani S. *Modélisation des différentes technologies d'éoliennes intégrées dans un réseau de moyenne tension*. PhD Dissertation, Ecole Centrale de Lille, 2004. (Fra).

Received 18.12.2021

Accepted 20.02.2022

Published 20.04.2022

*Abderraouf Boumassata*¹, Dr.,
*Djallel Kerdoun*², Professor,
*Oussama Oualah*², PhD Student,
¹Department of EEA, LGCEP-Laboratory,
 National Polytechnic School Constantine,
 BP 75, A, Nouvelle ville RP, Constantine, Algeria,
 e-mail: a_boumassata@umc.edu.dz (Corresponding Author)
²Department of Electrotechnical, LGEC-Laboratory,
 Brothers Mentouri University Constantine 1,
 Compus Ahmed Hamani, Zarzara, Constantine, Algeria,
 e-mail: Kerdjallel@yahoo.fr, oussama.oulha@umc.edu.dz

How to cite this article:

Boumassata A., Kerdoun D., Oualah O. Maximum power control of a wind generator with an energy storage system to fix the delivered power. *Electrical Engineering & Electromechanics*, 2022, no. 2, pp. 41-46. doi: <https://doi.org/10.20998/2074-272X.2022.2.07>